Report Title:

ACTIVE CATHODES FOR SUPER-HIGH POWER DENSITY SOLID OXIDE FUEL CELLS THROUGH SPACE CHARGE EFFECTS

Type of Report: Quarterly Technical Report

Reporting Period Start Date: April 1, 2003
Reporting Period End Date: June 30, 2003
Principal Author: Professor Anil V. Virkar
Date Report was Issued: November 3, 2003
DOE Award Number: DE-FC26-02NT41602

Name and Address of Submitting Organization:

Department of Materials Science & Engineering
122 S. Central Campus Drive
University of Utah
Salt Lake City, UT 84112

DISCLAIMER:

ABSTRACT

This report summarizes the work done during the third quarter of the project. Effort was directed in two areas: (1) Further development of the model on the role of connectivity on ionic conductivity of porous bodies, including the role of grain boundaries, and its relationship to cathode polarization. Included indirectly through the grain boundary effect is the effect of space charge. 2) Synthesis of LSC + SDC composite cathode powders by combustion synthesis. (3) Fabrication and testing of anode-supported single cells made using synthesized LSC + ScDC composite cathodes.

TABLE OF CONTENTS

INTRODUCTION

It is known that electrode transport properties and morphology have a profound effect on electrode polarization and thus on solid oxide fuel cell (SOFC) performance [1-4]. Recent work has shown that a large part of the polarization loss is associated with the cathode [5,6]. In addition to the morphological effect, it is also known that ionic conductivity of the cathode has a large effect on cathodic polarization. It is assumed that the electronic conductivity of the cathode is high enough not to be a limiting factor. This is usually a good assumption with materials such as LSM and LSC, which have electronic conductivities over the temperature of interest between ~200 and 1000 S/cm. By contrast, the ionic conductivity of either YSZ or ceria or LSGM is well below 1 S/cm at similar temperatures. Even with the possible use of bismuth oxide for the cathode, the ionic conductivity is still much lower than the electronic conductivity. The grain size also has a large effect on conductivity [7]. It is desired that the cathode microstructure close to the electrolyte be as fine as possible. When the particle size is very fine, there can be a significant effect of space charge on transport [8-13]. The effect of space charge can be potentially quite large in ionic conductors. It could either increase conductivity, or could decrease it. It is desired that the space charge be such that it enhances ionic conductivity of porous bodies. It is possible, however, that space charge effects are actually detrimental. In such a case, the approach should be to seek to lower these effects – assuming this is possible. One area in which space charge effects can be significant is the effect of grain size on conductivity. As part of this work, therefore, effect of grain size on cathode polarization will be examined in the future. In this report, theoretical analysis of the ionic conductivity of porous bodies is extended to include the effects of grain boundaries. It is to be noted that the principal factor, which leads to the grain boundary effect is the presence of space charge, assuming grain boundaries are devoid of secondary phases. If secondary phases are present, then there will be contribution from them as well. In this report, results of experiments on composite cathode powder synthesis, and fabrication and testing of anode-supported single cells made using the synthesized cathodes, are also described. The results show that the composition of ScDC, the ionic conductor in the composite cathode, has a significant effect on cell performance – which is a direct result of the effect of ScDC composition on cathode polarization.

EXECUTIVE SUMMARY

Solid oxide fuel cells (SOFC) can operate over a wide temperature range, from ~600 to 1000^{o}C, and can use a variety of hydrocarbon fuels, once appropriately processed. The current target for SOFC is about 800^{o}C, although efforts are presently underway to lower the operating temperature below 700^{o}C. The largest voltage loss (polarization) in SOFC is known to occur at the cathode. There are two types of cathodic polarizations: (1) Concentration polarization – that associated with gas transport. (2) Activation polarization – that associated with the occurrence of the overall electrochemical cathodic reaction of charge transfer. The former is relatively small, as long as the cathode is thin and has sufficient porosity [14]. The latter is the dominant one, and depends upon a number of microstructural and intrinsic – fundamental, parameters. This research aims to address cathodic activation polarization. Specifically, this research aims to lower the cathodic polarization through cathode modification through space charge effects. Our prior work has shown that the effective cathodic polarization resistance depends upon the following factors. (1) The particle size of the ionic conductor in a composite cathode, comprising a two phase, porous, contiguous mixture of an ionic conductor and an electrocatalyst – the latter being an electronic conductor. In general, the smaller the particle size of the ionic conductor, the lower is the cathodic activation polarization. (2) The ionic conductivity of the ionic conductor also has a significant effect – the higher the ionic conductivity, the lower is the cathodic polarization. (3) Intrinsic charge transfer resistance – the lower the intrinsic charge transfer resistance, the lower is the cathodic activation polarization.

The above factors themselves depend upon some other fundamental parameters. It is known that in the majority of the ionic conductors, the smaller the grain size, the higher is the net resistivity. This is attributed to grain boundaries, which usually offer resistance to ion transport. Part of this resistance is attributable to space charge effects, which in some materials (e.g. YSZ) tend to lower oxygen vacancy concentration near grain boundaries. Depending upon the dopant type and amount, it is in principle possible to actually enhance the oxygen vacancy concentration near grain boundaries. If this can be achieved, significant lowering of cathodic polarization can occur. This research aims to identify fundamental parameters, which tend to increase oxygen vacancy concentration near grain boundaries. This is expected to depend upon the chemistry of the material as well as processing.

The other factor involves the nature of inter-particle necks. If the contact between particles is poor (small), the overall resistance can be large, leading to high cathodic polarization. During the previous reporting periods, the effect of inter-particle neck size on total conductivity of porous bodies was theoretically analyzed, and experimental results were presented. The results showed that the neck size between particles has a profound effect on ionic conductivity. Specifically, it was shown that for highly porous samples of identical porosities (~50%), the absolute value of conductivity was ~75 times higher in samples with sufficiently large neck sizes (good connectivity) as compared to samples with small neck sizes (poor connectivity). It is to be noted that this has profound influence on cathode polarization. The theoretical calculation presented did not include grain boundary effects. In this report, the analysis is extended to include grain boundary effects. The analysis shows that the effect of grain boundaries is quite large, and the term containing the grain boundary effect becomes

singular faster than the bulk term as the neck size becomes smaller (as $\alpha \to 0$), where α is the relative neck size. In future work, the objective will be to obtain an experimental estimate of the α through quantitative stereology. In this report, results on composite cathode synthesis and fabrication and testing of anode-supported single cells with composite cathodes are presented. In later work, the objective will be to conduct quantitative stereological analysis of cathodes, and relate performance of cells (cathodic polarization) to cathode microstructure – with emphasis on the role of α. In the area of modeling, the future work will include the effect of neck size and grain boundary effect when the space charge enhances ionic conduction.

EXPERIMENTAL

During this reporting period, efforts were directed in the following areas.

1. Extension of the theoretical analysis of ionic conduction in porous bodies, including the role of grain boundaries.
2. Synthesis of fine powders of strontium doped lanthanum cobaltite (LSC). The following procedure was used. Cobalt (II) nitrate hexahydrate $Co(NO_3)_2.6H_2O$, lanthanum (III) nitrate hexahydrate $La(NO_3)_3.6H_2O$ and strontium (II) nitrate $Sr(NO_3)_2$ were mixed in requisite proportions corresponding to a single phase LSC peroskite composition, and dissolved in de-ionized water. Then di-gluconic acid (DGA) was added in the required amount. The solution was heated in a stainless steel beaker on a hot plate. Once all of the water was vaporized, the mixture combusted, resulting in rapid rise in temperature. The temperature was recorded by a thermocouple. The measured temperature was, however, much lower than the calculated adiabatic flame temperature. The resulting product was a very fine powder.
3. Two phase mixtures of samaria-doped ceria (SDC) and LSC were also prepared by combustion synthesis. The experimental process is the same as that discussed above. The precursors used were cobalt (II) nitrate hexahydrate $Co(NO_3)_2.6H_2O$, lanthanum (III) nitrate hexahydrate $La(NO_3)_3.6H_2O$, strontium (II) nitrate $Sr(NO_3)_2$, samarium nitrate, $Sm(NO_3)_3$, and cerium nitrate, $Ce(NO_3)_3$. The powder was characterized by X-ray diffraction (XRD).
4. Button cells with composite cathodes of LSC and ScDC, containing varying mole percent of samaria between 20% and 40%, were made: Anode supported cells comprising a Ni/YSZ anode support, a Ni/YSZ anode interlayer, a thin film YSZ electrolyte, and ScDC barrier layer were fabricated using standard ceramic processing techniques. The difference between the three cells is that ceria in the composite cathode contained different amounts of scandia as a dopant. The cells were tested at 800^oC with hydrogen-air.

RESULTS AND DISCUSSION

The Effect of Grain Boundaries on Ionic Conductivity of Porous Bodies: The Effect of Space Charge: Recent work by Guo [9] has shown that in YSZ, the grain boundary resistivity can be attributed to a space charge region (depletion of oxygen vacancies), which appears near grain boundaries. In principle, the grain boundary space charge region can either enhance or suppress ionic conduction. If the space charge region has a positive effect (enhancement in ionic conduction), cathodes should be designed to exhibit greater grain boundary regions (lower the grain size). If the space charge region suppresses ionic conduction, then the approach should be to minimize the grain boundary effect through compositional and microstructural modifications. In YSZ, the grain boundary region is depleted in oxygen vacancy concentration, which effectively leads to an increase in the grain boundary resistance. This effect must also be taken into account

when analyzing, and designing composite cathodes. Earlier, we examined the problem of conduction in porous bodies, in which the effect of neck size on the effective resistivity was not taken into account. This calculation showed that net effective resistivity is a function of the relative neck size, α, where $\alpha = r_o / R$. In that calculation, the role of grain boundary resistance was not included. As stated above, in most oxygen ion conductors, it is known that the grain boundary resistivity cannot be neglected. In fact in many cases, it can be quite large. Relevant parameters, which determine transport across a grain boundary are, ρ_{gb}, grain boundary resistivity, and δ_{gb}, grain boundary thickness. It is generally not possible to separate the two, and one speaks of $\rho_{gb}\delta_{gb}$ as the grain boundary area specific resistance in Ωcm^2. This parameter depends upon the space charge layer (defect concentrations and thickness), and may either increase or decrease the product $\rho_{gb}\delta_{gb}$. The following analysis is for a composite cathode, a schematic of which is shown in Figure 1. The analysis focuses on one pillar (shown without the electrocatalyst particles in Figure 2). In what follows, it is assumed that each sphere is a single grain. In many cases, this need not be true. That is each sphere may actually contain many grains. In such a case, it would be necessary to include this aspect when considering ionic transport through the spheres (particles).

The following is an analysis for spherical grains of radius R, and neck size of r_o, arranged as a pillar (one dimensional) shown in Figure 2. The geometry is shown in Figure 3. Figure 3(a) shows two grains in the pillar, with a grain boundary in between. Figure 3(b) shows a half of the grain with half of the grain boundary associated with it. This is the geometry used in the calculations.

The analysis shows that the effective resistivity as a function of the relative neck size α including the neck size, is given by

$$\rho_{eff} = \frac{\rho_g}{2\sqrt{1-\alpha^2}} \ln\left\{\frac{1+\sqrt{1-\alpha^2}}{1-\sqrt{1-\alpha^2}}\right\} + \frac{\rho_{gb}\delta_{gb}}{2R\alpha^2\sqrt{1-\alpha^2}} \qquad (1)$$

The preceding equation shows that the effective ionic resistivity of a porous ionic conductor depends on the grain resistivity, ρ_g, the grain boundary resistivity parameter, namely $\rho_{gb}\delta_{gb}$, and the relative neck size, α, given by $\alpha = r_o / R$. Of particular interest is to determine the relative contributions of the two terms as a function of α for small values of α. Note that as $\alpha \to 0$, both of the terms go to infinity (become singular). Our interest is in determining which of the terms goes to infinity faster as $\alpha \to 0$. It is readily shown that as $\alpha \to 0$, the above equation can be approximately given by

$$\rho_{eff} \approx \frac{\rho_g}{2} \ln\left(\frac{2}{\alpha}\right) + \frac{\rho_{gb}\delta_{gb}}{2R\alpha^2} \qquad (2)$$

As seen from equation (2), as $\alpha \to 0$, both terms become infinite. One can use l'Hospital's rule to show that the second term goes to infinity faster. Ratio of the derivatives of the second term to the first varies as $1/\alpha^2$. This result has significant implications concerning the ionic resistivity of porous bodies, the role of grain

boundaries, and the cathodic polarization resistance of composite (or single-phase) MIEC cathodes. That is, a poorly sintered cathode (with narrow necks) will exhibit high ρ_{eff}, and thus high polarization resistance. The role of grain boundaries is actually disproportionately high on ρ_{eff}, due mainly to small neck sizes. The effective cathodic polarization of composite cathodes is given by

$$R_{ct(eff)} \approx \sqrt{\frac{2\rho_{eff} R_{ct} R}{(1-V_v)}} = \sqrt{\frac{2\rho_{eff}\rho_{ct} R}{(1-V_v) l_{TPB}}} \qquad (3)$$

A high ρ_{eff} leads to a high $R_{ct(eff)}$. If the space charge effect is such as to enhance the oxygen vacancy concentration near the grain boundaries, the ρ_{eff} will be lower, and the effective polarization resistance will also be lower. If, however, the space charge effect is to lower oxygen vacancy concentration near the grain boundaries, such as is the case in YSZ, the effective polarization resistance will be higher. In such cases, the need for good inter-particle contact cannot be overemphasized.

Synthesis of Nanosize Powders of LSC and Two-Phase Mixtures of SDC and LSC:

Very fine (nanosize) particles are preferred, especially if the grain boundary effect is not dominant. In addition, the electrocatalyst and ionic conductor particles from composite cathodes should be as well dispersed as possible. For this reason, effort was initiated on the synthesis of LSC + SDC powder mixtures by combustion synthesis. Figure 4 shows an XRD trace of the as-synthesized LSC powder. Note that the peak width is quite large, indicating very small (nanosize) crystallite size. XRD trace of an LSC sample calcined at 1100^{o}C for 2 hours is shown in Figure 5. The structure corresponds to that of a perovskite. Note that the peaks are quite sharp and narrow, consistent with the occurrence of significant particle growth during calcining.

Figure 6 shows a mixture of two phases with varying ratios of SDC to LSC, namely 40:60, 50:50 and 60:40. For comparison, pure LSC and SDC patterns are also shown in Figure 6.

Evaluation of Cell Performance with Composite LSC + ScDC Cathodes with ScDC Containing Scandia between 20% and 40%:

Initial work was initiated on ScDC powders since Sc has a relatively small ionic size, and would have a lower tendency for segregation near free surfaces. Synthesis of ScDC powders was described in earlier reports. The cells were tested at 800^{o}C with hydrogen as fuel and air as the oxidant. Figure 7 shows the performance curves. The highest performance was measured to be ~1.78 W/cm^2. Note that the performance is the highest with composite cathode with ScDC containing 40% scandia, and the lowest with ScDC containing 20% scandia. It is expected that ionic conductivity of ScDC with 40% scandia would be higher due to the higher oxygen vacancy concentration. Note that the area specific resistance (ASR) of the cell varies between 0.128 Ωcm^2 and 0.144 Ωcm^2. This difference of 0.016 Ωcm^2 is attributed to the difference in the compositions of ScDC in the composite cathodes. In the future, attempts will be made to quantitatively characterize

the microstructures to determine the particle and the neck sizes, and also measure porosity.

CONCLUSION

In the first quarterly report, a simple analytical equation was derived, which describes the conductivity as a function of connectivity. In the second quarterly report, experimental evidence was presented on the role of connectivity on ionic conductivity. It was observed that the connectivity has a large effect on conductivity of porous bodies. In this report, the model was extended to include the effect of grain boundaries forming at the necks between particles. It was assumed that the particles are single crystalline. However, if particles are aggregates of grains, then it would be necessary to replace ρ_g from equations (1) and (2) by $\rho_g + \alpha \frac{\rho_{gb}\delta_{gb}}{d}$, where d is the grain size and that $d << 2R$, where R is the particle size. For the case considered here, it was shown that the effect of grain boundaries can be very large. Thus, efforts must be made to enhance the neck size. The model shows that as the neck size decreases, the term containing grain boundary effects becomes singular faster than the bulk term. The case analyzed here corresponds to that in which grain boundaries hinder ionic transport. Such is the case with YSZ, in which within the space charge region adjacent to grain boundaries, the oxygen vacancy concentration is lower than that in the bulk. Future models will address cases in which within the space charge layer, oxygen vacancy concentration is higher than in the bulk. Experimental challenge will be to identify dopants for zirconia or ceria (or other ionic conductors), in which space charge enhances ionic conduction. Experimental work was done on the synthesis of LSC + SDC composite cathodes by combustion synthesis. In the future, cells will be made with SDC-based composite cathodes. Anode-supported cells were made with different compositions of ScDC in the cathode. The ScDC powders were made during the earlier period. It was observed that the cell performance was the highest when the scandia content in the ScDC was the highest, consistent with the expectation of highest ionic conductivity of the materials tested here. Ionic conductivity measurements will be carried out on porous ScDC with different scandia contents in the future to determine if the hypothesis is correct.

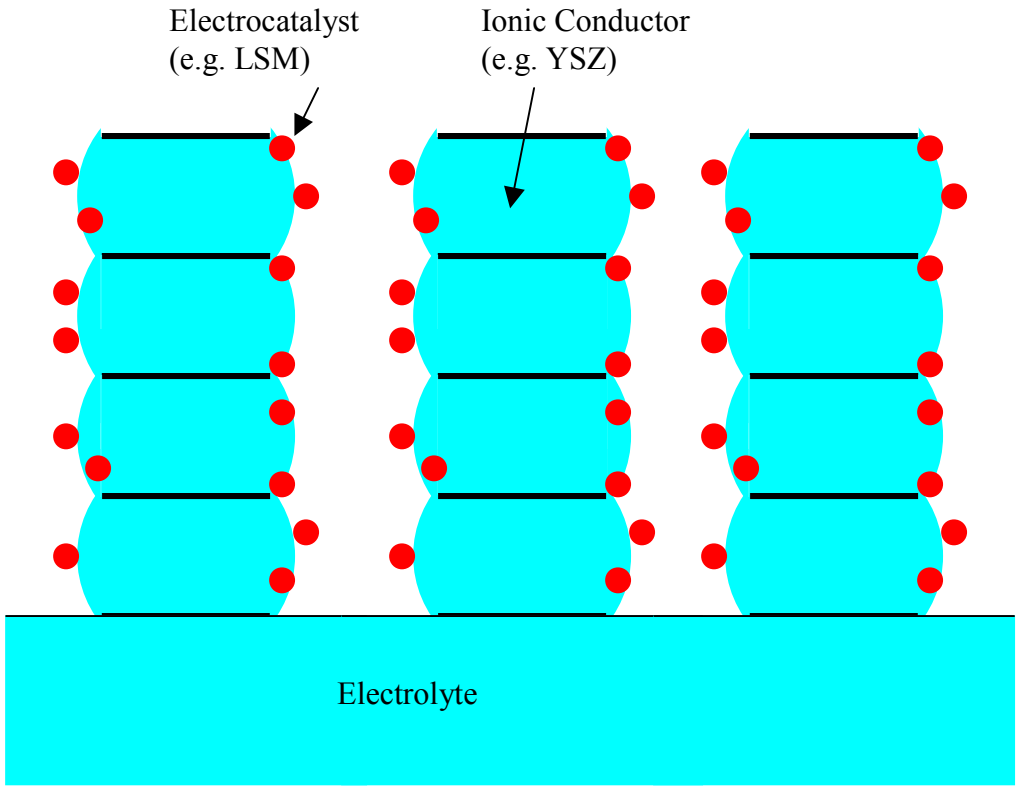

Figure 1: A schematic of a composite cathode. The electrocatalyst particles are in physical contact with neighboring particles – not isolated. The two-dimensional cutout gives an appearance of their being isolated. There also is a significant amount of connected porosity and three-phase boundary (TPB) length.

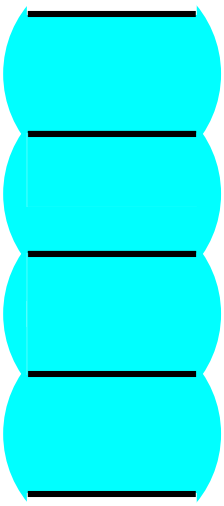

Figure 2: A schematic of an isolated pillar.

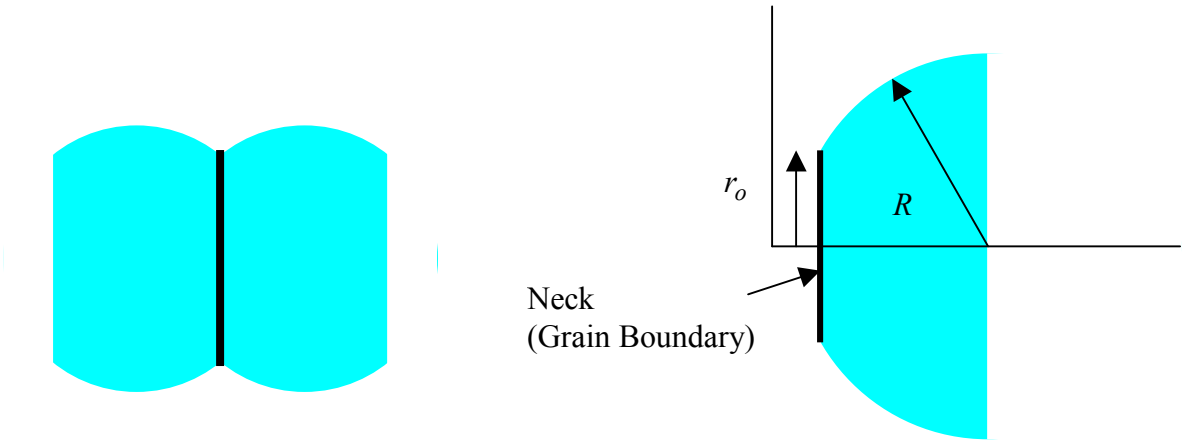

<u>Figure 3:</u> (a) Two adjacent grains (it is assumed here that they are grains, although in principle, they could be agglomerates of grains. If they are agglomerates, then the effect of intraparticle grain boundaries must also be accounted for.) from the pillar with a grain boundary in between. (b) The geometry used for calculations.

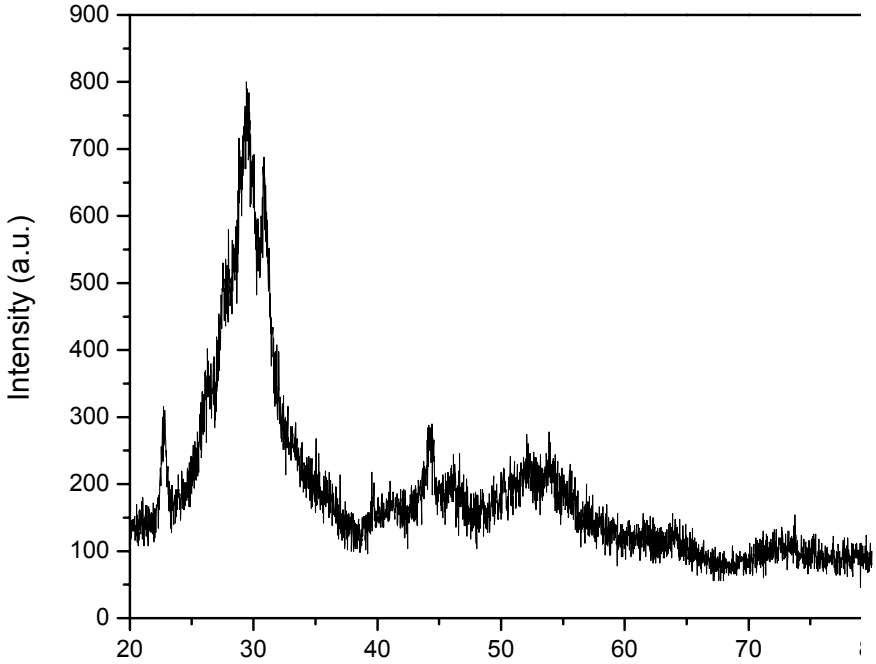

<u>Figure 4:</u> An XRD pattern of strontium-doped lanthanum cobaltite (LSC) formed by combustion synthesis. Note the large peak width, indicative of nanosize of the powder formed.

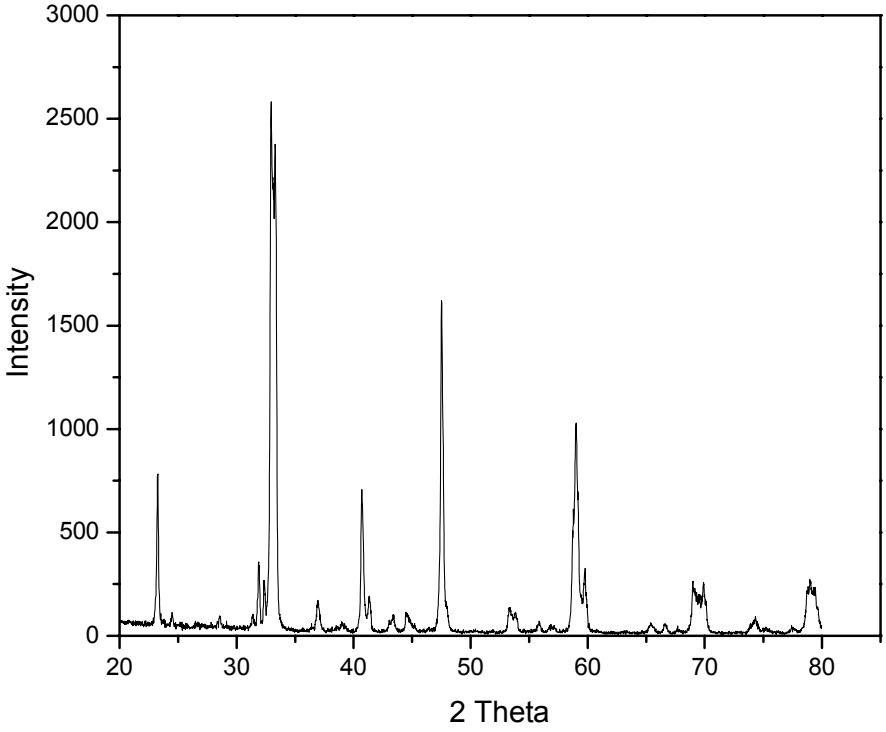

Figure 5: XRD patterns of strontium-doped lanthanum cobaltite (LSC) formed by combustion synthesis and calcined at 1100°C for 2 hours. Note the small peak width, indicative of growth of particles during calcining.

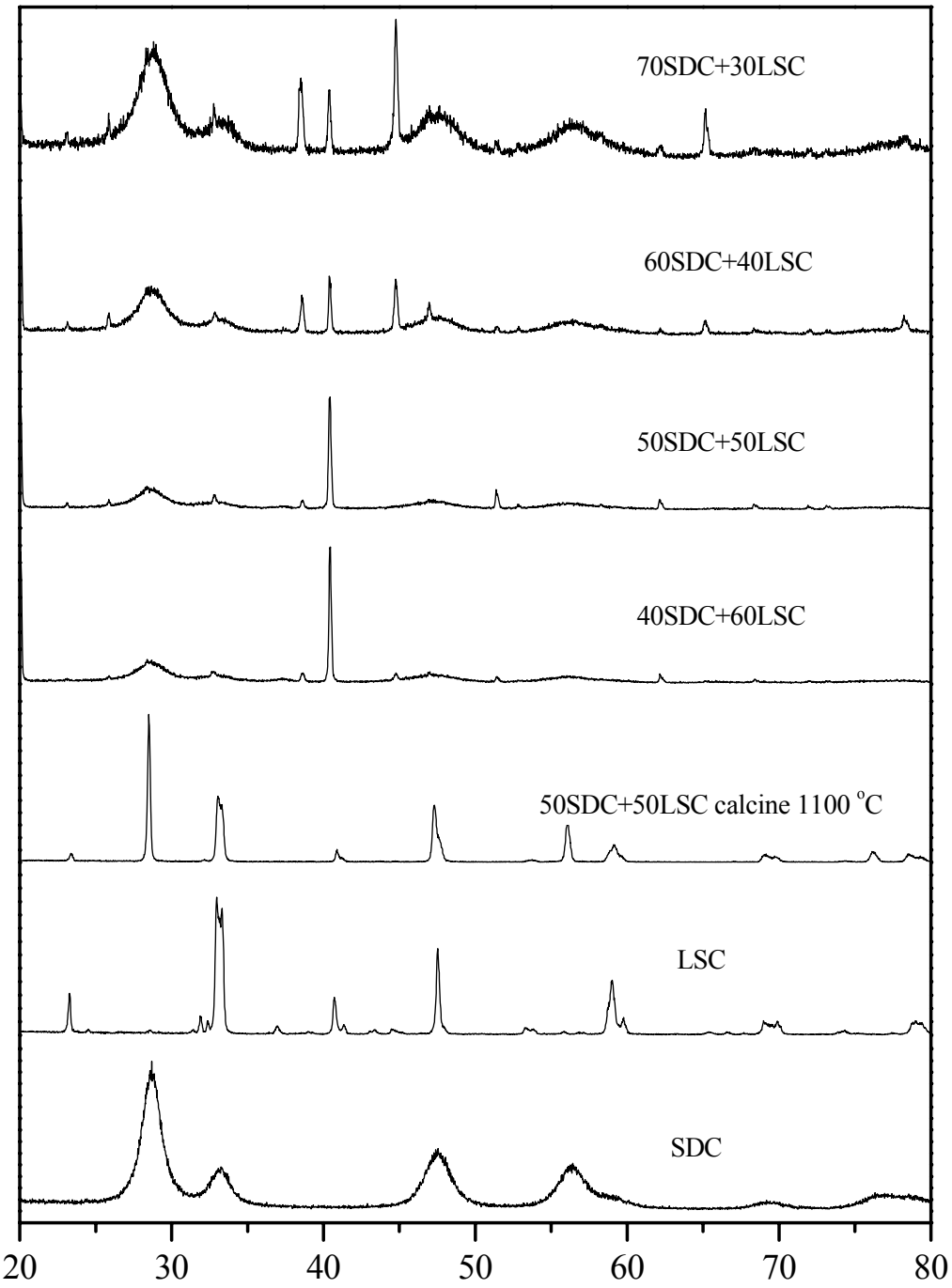

Figure 6: Comparison of XRD patterns of strontium-doped lanthanum cobaltite (LSC) and Sm-doped CeO_2 (SDC) with two-phase mixtures of SDC and LSC formed by combustion synthesis.

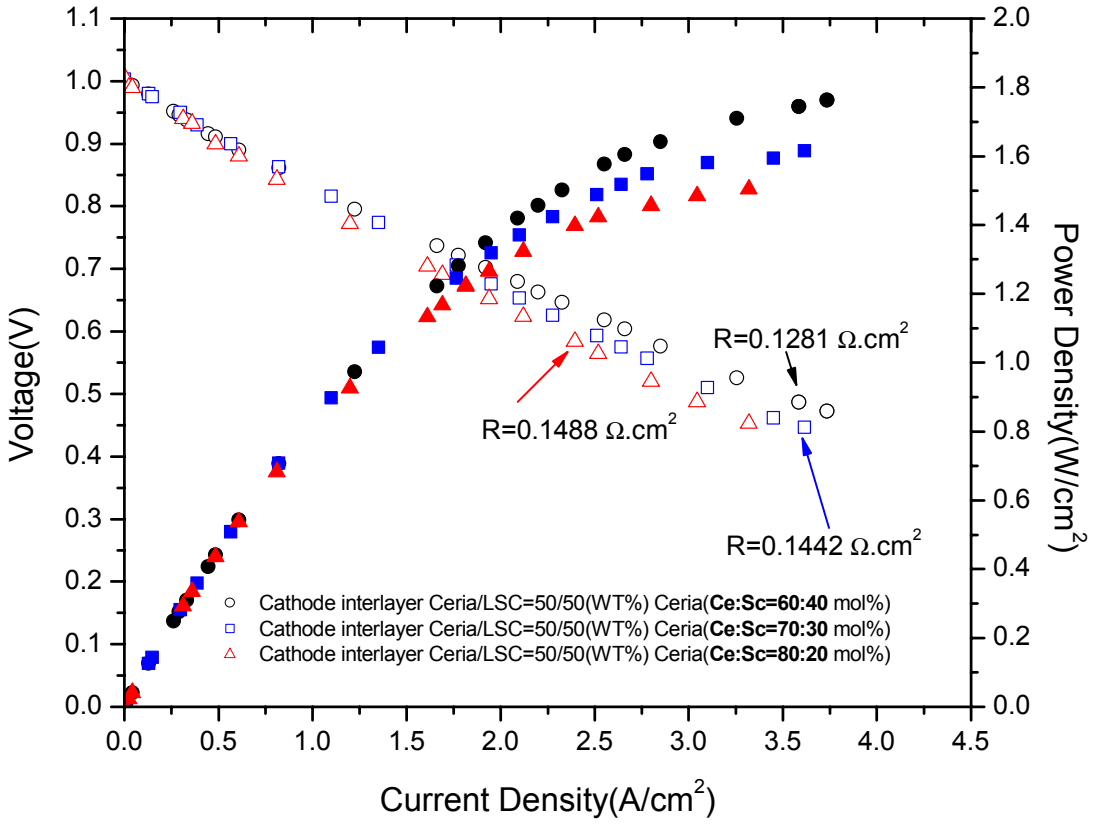

Figure 7: Voltage and power density vs. current density for anode-supported cells with composite cathodes comprised of LSC + ScDC. Cells were tested at 800^{o}C with hydrogen as the fuel and air as the oxidant.

REFERENCES

1) T. Kenjo, S. Osawa, and K. Fujikawa, *J. Electrochem. Soc*., **138** 349 (1991).
2) C. W. Tanner, K-Z. Fung, and A. V. Virkar, *J. Electrochem. Soc*., **144** 21-30 (1997).
3) H. Deng, M. Zhou, and B. Abeles, *Solid State Ionics*, **74** 75 (1994).
4) I. V. Murygin, *Elektrokhimiya*, **23** [6] 740 (1987).
5) A. V. Virkar, J. Chen, C. W. Tanner, and J-W. Kim, *Solid State Ionics*, **131** 189 (2000).
6) F. Zhao, Y. Jiang, G-Y. Lin, and A. V. Virkar, pp. 501 in SOFC VII, edited by H. Yokokawa and S. C. Singhal, Electrochemical Society Publication, Pennington, NJ, (2001).
7) M. J. Verkerk, B. J. Middlehuis, and A. J. Burggraaf, *Solid State Ionics*, **6** 159 (1982).
8) X. Guo, *Solid State Ionics*, **81** 235-242 (1995).
9) X. Guo, *Solid State Ionics*, **99** 137-142 (1997).
10) J. Frenkel, p. 37 in 'Kinetic Theory of Liquids', Dover, NY (1946).
11) K. Lehovec, *J. Chem. Phys*., **21** [7] 1123-1128 (1953).
12) K. L. Kliewer and J. S. Koehler, *Phys. Rev*., **140** [4A], A1226-A1240 (1965).
13) K. L. Kliewer, *Phys. Rev*., **140** [4A], A1241-A1246 (1965).
14) F. Zhao, T. Armstrong, and A. V. Virkar, *J. Electrochem. Soc*., **150** [3] A249-A256 (2003).

LIST OF ACRONYMS AND ABBREVIATIONS

ASR:	Area specific resistance
DC:	Direct current
DGA:	Di-gluconic acid
LSC:	Sr-doped $LaCoO_3$
LSGM:	Sr- and Mg-doped $LaGaO_3$
LSM:	Sr-doped $LaMnO_3$
SDC:	Samaria-doped ceria
ScDC:	Scandia-doped ceria
SEM:	Scanning electron microscopy
SOFC:	Solid oxide fuel cell
TPB:	Three-phase boundary
XRD:	X-ray diffraction